Biochimica et Biophysica Acta 1850 (2015) 281–286

Contents lists available at ScienceDirect

Biochimica et Biophysica Acta

journal homepage: www.elsevier.com/locate/bbagen

Mechanism of dopachrome tautomerization into 5,6-dihydroxyindole-2-carboxylic acid catalyzed by Cu(II) based on quantum chemical calculations

Ryo Kishida [a], Adhitya G. Saputro [a], Hideaki Kasai [a,b,*]

[a] Department of Applied Physics, Osaka University, Suita, Osaka, Japan
[b] Center for Atomic and Molecular Technologies, Osaka University, Suita, Osaka, Japan

ARTICLE INFO

Article history:
Received 3 August 2014
Received in revised form 18 October 2014
Accepted 21 October 2014
Available online 28 October 2014

Keywords:
Dopachrome
DHICA
Melanin
Eumelanin
Copper
Density functional theory

ABSTRACT

Background: Tautomerization of dopachrome to 5,6-dihydroxyindole-2-carboxylic acid (DHICA) is a biologically crucial reaction relevant to melanin synthesis, cellular antioxidation, and cross-talk among epidermal cells. Since dopachrome spontaneously converts into 5,6-dihydroxyindole (DHI) via decarboxylation without any enzymes at physiologically usual pH, the mechanism of how tautomerization to DHICA occurs in physiological system is a subject of intense debate. A previous work has found that Cu(II) is an important factor to catalyze the tautomerization of dopachrome to DHICA. However, the effect of Cu(II) on the tautomerization has not been clarified at the atomic level.

Methods: We propose the reaction mechanism of the tautomerization to DHICA by Cu(II) from density functional theory-based calculation.

Results: We clarified that the activation barriers of α-deprotonation, β-deprotonation, and decarboxylation from dopachrome are significantly reduced by coordination of Cu(II) to quinonoid oxygens (5,6-oxygens) of dopachrome, with the lowest activation barrier of β-deprotonation among them. In contrast to our previous work, in which β-deprotonation and quinonoid protonation (O5/O6-protonation) were shown to be important to form DHI, our results show that the Cu(II) coordination to quinonoid oxygens inhibits the quinonoid protonation, leading to the preference of proton rearrangement from β-carbon to carboxylate group but not to the quinonoid oxygens.

Conclusion: Integrating these results, we conclude that dopachrome tautomerization first proceeds via proton rearrangement from β-carbon to carboxylate group and subsequently undergoes α-deprotonation to form DHICA.

General significance: This study would provide the biochemical basis of DHICA metabolism and the generalized view of dopachrome conversion which is important to understand melanogenesis.

1. Introduction

Melanins, one of the most important pigments in animals, are known to have various functions that are essential for living organisms. The biosyntheses of melanins mainly occur in the melanosomes, membrane bound organelles within pigment cells such as melanocytes which are distributed in the epidermis, the hair follicle, the inner ear, and the eye [1–4]. Biosynthesized melanins consist of two distinct pigments, black to brown eumelanins and yellow to reddish-brown pheomelanins [5–10]. Especially, the photoprotective and antioxidative effects of eumelanins have extensively been investigated as major functions although the high photosensitizing effects of pheomelanins have been considered to confer cytotoxicity [11]. Neuromelanins, melanin-like pigments which are mainly found in the neurons of substantia nigra and locus coeruleus, have also been recognized to play important physiological roles such as sequestration of heavy metal ions and methylphenylpyridine (MPP^+) which is known to cause the Parkinson's disease [12,13]. Although the biological and medical relevance of melanins and their biosyntheses have been subject to controversy [14,15], it is well accepted that eumelanins have an ability to convert absorbed light energy into heat energy [16–18] and to detoxify reactive oxygen species (ROS) [19–21].

Eumelanins are basically recognized as stacked and aggregated oligomers or large heteropolymers that are mainly composed of two monomers, 5,6-dihydroxyindole (DHI) and 5,6-dihydroxyindole-2-carboxylic acid (DHICA) [22–24]. The biosynthesis of DHICA is achieved by tautomerization of dopachrome, an intermediate in melanogenesis (Fig. 1) [25,26]. Dopachrome is a comparatively unstable molecule

* Corresponding author at: Tel.: +81 6 6879 7857; fax: +81 6 6879 7859.
E-mail addresses: kasai@dyn.ap.eng.osaka-u.ac.jp, kasai@dyn.ap.eng.osaka-u.ac.jp (H. Kasai).

http://dx.doi.org/10.1016/j.bbagen.2014.10.024
0304-4165/

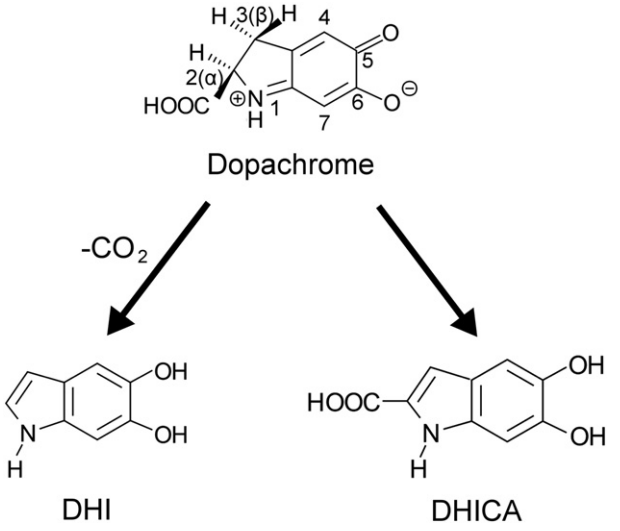

Fig. 1. Conversion of dopachrome to DHI and DHICA via decarboxylative route and tautomerization route, respectively. Labels in this figure denote the position for each carbon and nitrogen atom corresponding to usual chemical nomenclature.

that slowly converts to DHI via decarboxylation without any enzymes at physiologically usual pH (Fig. 1) [27,28]. Due to this nature of dopachrome, eumelanin had been initially considered to consist mostly of DHI in early research on melanin chemistry. However, this view was reconsidered by analyses mainly based on chemical degradation that natural eumelanins include DHI and DHICA units at a nearly equal ratio [29].

In an experiment, it was demonstrated that DHICA units in eumelanin are responsible for the antioxidative properties of the pigment [30]. As well as eumelanin itself, DHICA and its methoxy metabolite, 6-hydroxy-5-methoxyindole-2-carboxylic acid (6H5MICA) were also found to exhibit considerable antioxidant activity [31]. Recently, it was also reported that DHICA affects cross-talk among epidermal cells, implying the pivotal roles of this molecule in skin homeostasis and cell-protection [32]. These evidences strongly show the physiological significance of DHICA metabolism.

Experimental works have found some key factors to tautomerize to DHICA; divalent metal ions, especially Cu(II) [33–35], and dopachrome tautomerase (DCT), which contains a pair of Zn(II) ions at its active sites [36–38], can strongly catalyze the tautomerization of dopachrome. Although the effect of Zn(II) itself on the tautomerization has shown to be considerably weaker than that of Cu(II) [33], DCT is significantly potent in catalyzing the reaction. A comparative study of the tautomerization effect between DCT and Cu(II) revealed that DCT is more intensive to catalyze the tautomerization than Cu(II) [39]. This result may give us an impression that the effect of Cu(II) is not a major factor for DHICA formation. However, although DCT expression in human follicular melanocytes from elderly individuals had been shown to be scarcely detectable [40], chemical degradation analyses clarified that these samples contain a relatively high ratio of DHICA (33–45%) [41,42]. Therefore, a reappraisal of the contribution of Cu(II) towards the DHICA formation might afford a new understanding of melanin synthesis.

Experimental findings mentioned above trigger us to ask further question about the mechanisms of how these factors selectively tautomerize dopachrome. Previously, we clarified the mechanism of dopachrome conversion towards DHI formation based on the results obtained from first-principles calculation [43]. In this connection, the mechanistic difference of DHI/DHICA formation deserves attentions as a means of obtaining the generalized view of dopachrome conversion. A proposed mechanism of the DCT-catalyzed reaction may clearly explain the selectivity towards the formation of DHICA over DHI. According to the strong stereospecificity of DCT, an involvement of an interaction between carboxylate group of dopachrome and an unidentified group of DCT in the catalysis of DCT has been suggested as well as the participation of Zn(II) ions [38]. In this picture, the selective formation of DHICA will be described in terms of inhibition of decarboxylation, that leads to the reduction of the DHI formation. However, the clear pictures of the metal ions-catalyzed conversions have been poorly established despite the biological importance. Although metal ions are supposed to exert their catalytic activities to the tautomerization by interacting with quinonoid oxygens (5,6-oxygens, see Fig. 1) of dopachrome [33], the reason why such interactions could realize the selective formation of DHICA is unclear.

To obtain the clear-cut view of the formation of DHICA catalyzed by Cu(II), we consider a paired Cu(II)-dopachrome interacting system as a minimal model that would result in exclusive DHICA formation from dopachrome. Since the metal ions-catalyzed reactions are known to proceed by first-order kinetics [33], this modeling is consistent with the relevant experimental systems. Using this model, we present a theoretical evaluation of dopachrome conversion catalyzed by Cu(II). To gain a reliable description based on universally defined energy profile along the reaction pathway, we employ a density functional theory-based calculation.

Dopachrome conversion proceeds via three possible dissociations; α-deprotonation, β-deprotonation, and decarboxylation (Fig. 1). As can be understood by referencing the structures of the products, decarboxylation and α-deprotonation are respectively associated with the formation of DHI and DHICA. β-Deprotonation is accompanied with a formation of quinone methide intermediate (Fig. 2). From our calculations, we here show significant reductions of the activation barriers of α-deprotonation, β-deprotonation, and decarboxylation from dopachrome by coordination of Cu(II) to quinonoid oxygens (5,6-oxygens) of dopachrome, with the lowest activation barrier of β-deprotonation among them. As demonstrated in our previous work [43], β-deprotonation and quinonoid protonation (O5/O6-protonation) are important to form DHI. However, our results obtained in this work showed that the Cu(II) coordination to quinonoid oxygens inhibits the quinonoid protonation, leading to the preference of proton rearrangement from β-carbon to carboxylate group but not to the quinonoid oxygens. Integrating these results, we conclude that dopachrome tautomerization first proceeds via proton rearrangement from β-carbon to the carboxylate group and subsequently undergoes α-deprotonation to form DHICA.

2. Computational methods

2.1. Density functional theory-based calculation

In this work, we performed first-principles calculations based on density functional theory [44,45] with the Becke's three-parameter hybrid functional [46] combined with the Lee–Yang–Parr correlation functionals [47] (B3LYP). Calculations were carried out with 6-31++G(d,p) basis set using the Gaussian 09 suite of programs [48].

2.2. Solvation model

To appropriately reflect the stabilization by the dielectric response of surrounding water molecules, we use the integral equation formalism

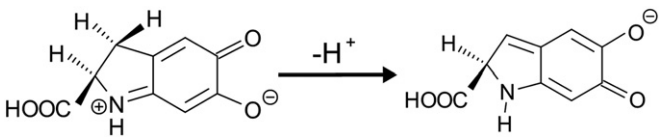

Fig. 2. Formation of quinone methide intermediate via β-deprotonation of dopachrome.

polarizable continuum model (IEF-PCM) [49], where the solvent molecules are modeled as a continuum medium whose dielectric constant is equal to that of the pure bulk solvent, and the solute molecule is placed within the cavity created in the dielectric medium. We also use the GePol algorithm [50] to make the cavity surface of the PCM smooth for the system including Cu(II). The reason why we use surface-smoothed cavity is that overlappings of van der Waals spheres between metal ion and ligands are small, giving clear difference of surface area between smoothed and non-smoothed cavity types.

In addition to the PCM, we explicitly consider peripheral water molecules around Cu(II) because water molecules participating the coordination bond with metal ions could affect the electronic state directly as described by the ligand field theory. 5-Fold coordination of Cu(II) aqua ion has been reported as the most preferable structure in aqueous solution [51,52]. However, considering the facts that the 5-fold solvation shell structure does not rigidly retain its structure but rapidly fluctuates [51], and that the out-of-plane coordination itself is weaker than the hydrogen bond in water cluster [52], we put only two water molecules to make a planer complex.

2.3. Coordination site for Cu(II)

We assume the quinonoid group as the major site for Cu(II) coordination although the carboxylate group may also bind with Cu(II). To check the validity of our assumption, we compare the thermodynamic preference of the two sites for Cu(II) coordination. Using the 4-fold coordination model for both two cases, we obtained the slightly lower Gibbs free energy of the quinonoid coordinated system with the free energy difference of −0.858 kcal/mol. Although the energy difference of two coordination systems is not significant, we do not focus on the carboxylate-coordinated system by Cu(II) because the Cu(II) coordination to the carboxylate cannot affect the activation barriers of α-deprotonation, β-deprotonation, as described in 3. Results and discussion section. Therefore, we focus on the quinonoid coordinated system in this paper although Cu(II) might collaterally act as a direct inhibitor of decarboxylation by coordinating to the carboxylate. The optimized structures of carboxyl-dissociated dopachrome with Cu(II) coordination to quinonoid group and carboxylate group are shown in Fig. 3 and Fig. S1 (in Supporting information), respectively.

2.4. Evaluation of activation energies

For the evaluations of activation energies of deprotonations and decarboxylation from dopachrome, we choose the dissociating bond length as the reaction coordinate, and assumed adiabatic relaxation of all other degrees of freedom unless the "rapid fluctuations" of the structure with the relaxation occur. Here, we define a rapid fluctuation as the variation of certain degrees of freedom with respect to reaction coordinate that cannot be reduced by reducing step size of the reaction coordinate. If the rapid fluctuations occur during evaluations of the dissociations, we use frozen values of the degrees of freedom from before the rapid fluctuation because such fluctuations are due to artificial error. Although such treatment may not satisfy the quantitative requirement, this assumption enables us to provide the well-defined values as the zeroth-order approximation.

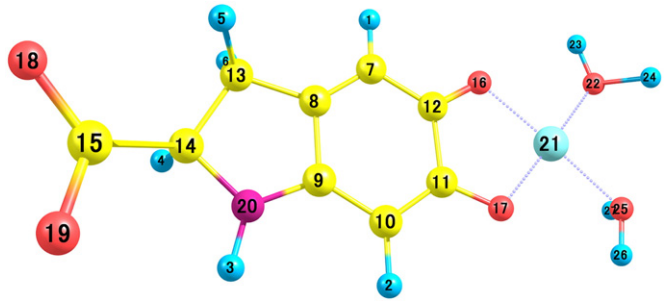

Fig. 3. Optimized structure (using the PCM) of carboxyl-dissociated dopachrome with Cu(II) coordination to quinonoid group. The blue, red, yellow, and purple spheres respectively represent hydrogen, oxygen, carbon, and nitrogen atom. Labels in this figure denote each atom, but do not correspond to the numbers used in usual chemical nomenclatures.

During the evaluations of activation energies, we put some water molecules to make hydrogen bonds with dissociating proton or carboxylate ion. As shown in Fig. 4, we choose water trimer and two water molecules for the proton and carboxylate ion, respectively. We found that the activation barrier of decarboxylation significantly varies depending on the presence/absence of the hydrogen bonds with the water molecules. Without hydrogen-bonded water molecules, we evaluated the activation barrier of decarboxylation to be 9.720 kcal/mol. This value is definitely smaller than that evaluated with the water molecules, 15.952 kcal/mol as shown in Fig. 5. The reason why these water molecules affect the activation energy can be attributed to the intramolecular electron transfer accompanied with decarboxylation; negative charges localized at oxygens of carboxylate are transferred to the π-conjugated system of dopachrome during decarboxylation. Therefore, such electron transfer will reduce the stabilization by the hydrogen bonds, leading to the higher activation barrier of decarboxylation than in the absence of the hydrogen bonds. We accordingly use the two water molecules bound to carboxylate ion for the realistic modeling. Although in this paper we compare the two cases with and without Cu(II) based on our present and previous results, the interaction between water molecules and carboxylate group was not explicitly considered in the previous calculations [43]. Nevertheless, we confirmed that inclusion of this interaction does not change the main conclusion because decarboxylation is still greatly activated by O5,O6-(di) protonation.

3. Results and discussion

3.1. Effect of Cu(II) on activation energies of α-deprotonation, β-deprotonation, and decarboxylation

First, we evaluate the activation energies of α-deprotonation, β-deprotonation, and decarboxylation from dopachrome in the presence of coordination of Cu(II) to quinonoid group. As described in the Introduction section, α-deprotonation, β-deprotonation, and decarboxylation are respectively associated with the formation of DHICA, quinone methide intermediate, and DHI. Thus, the comparison of activation energies of these dissociations will provide an essential information to understand the reaction mechanism. To evaluate the activation energies, we studied energy profiles along the dissociating bond lengths. As shown in Fig. 5, the activation energies of α-deprotonation, β-deprotonation, and decarboxylation are respectively 14.024 kcal/mol, 12.680 kcal/mol, and 15.952 kcal/mol. Note that the activation barrier of decarboxylation is obtained by using frozen value of dihedral angle around the cleaving C–C bond from before 1.81 Å of the bond length because the rapid fluctuation defined in 2. Computational methods section occurs at the point. This result indicates the kinetic preference of β-deprotonation compared with decarboxylation. All activation energies evaluated here are significantly lowered than those of the case without Cu(II) coordination as in the previous calculation [43]. This strong catalytic behavior of Cu(II) is consistent with experiments [33–35]. This catalysis might be explained as the consequence of stabilization of the α-deprotonated, β-deprotonated, and decarboxylated structures. From the natural population analysis [53], we found that each α-deprotonation, β-deprotonation, and decarboxylation leads to relatively large amount of electron transfer to the C–O bonds in the quinonoid group irrespective of the presence/absence of Cu(II) coordination, as shown in Table S1, S2 (in the Supporting Information). Since Cu(II) is positively charged, the coordination of Cu(II) will effectively contribute to the stabilization of the α-deprotonated,

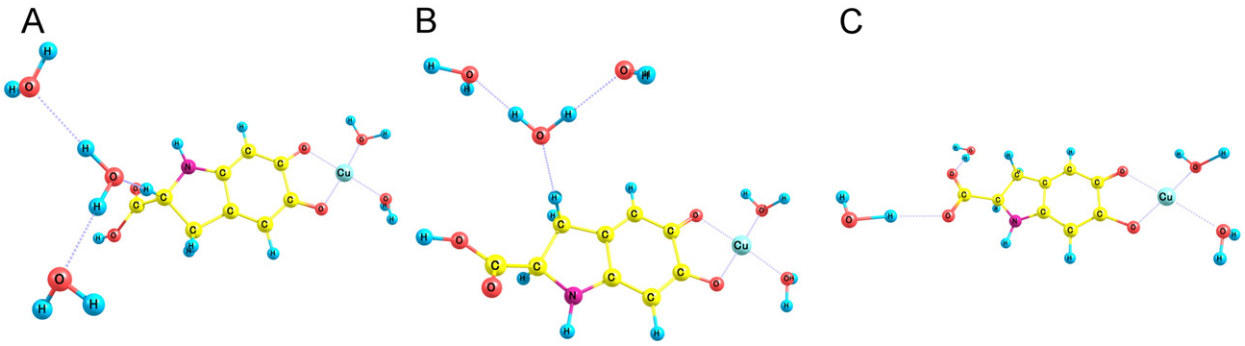

Fig. 4. Initial structures (optimized using the PCM) for (A) α-deprotonation, (B) β-deprotonation, and (C) decarboxylation of dopachrome with Cu(II) coordination to quinonoid group.

β-deprotonated, and the decarboxylated structures that have negatively charged 5,6-oxygens, leading to the reduction of activation barriers of these dissociations.

3.2. Cu(II) coordination to carboxylate group

As mentioned in 2. Computational methods section, we also examined the case of Cu(II) coordination to carboxylate group. We show the energy profiles along α-deprotonation and β-deprotonation with the carboxylate coordination of Cu(II) in Fig. 6. From Fig. 6, it can be seen that the energy profiles do not exhibit obvious transition state but exhibit plateau region similar to the cases in the absence of Cu(II) coordination, which were shown in our previous work [43]. The energy difference between the α-deprotonated and β-deprotonated structures compared with the initial structures can be estimated to 23.148 kcal/mol and 23.031 kcal/mol, respectively. Therefore, we can conclude that the carboxylate coordination of Cu(II) does not catalyze dopachrome conversion.

3.3. Proton rearrangement from β-carbon to other sites

From our results of the activation energies of α-deprotonation, β-deprotonation, and decarboxylation, we are able to see the preference of β-deprotonation compared with α-deprotonation and decarboxylation, indicating that the Cu(II)-catalyzed tautomerization of dopachrome also proceeds via the formation of quinone methide intermediate. To understand the second step of the tautomerization after β-deprotonation, we next examine the stabilities of possible intermediates. As the preferable sites for reprotonation after β-deprotonation, we consider the 5,6-oxygens of the quinonoid group and the carboxylate oxygen. In Table 1, we show the comparison of energetic stability for the each reprotonated structure in the presence/absence of Cu(II) coordination to the quinonoid group whose structures are shown in Supporting information Fig. S2. As shown in Table 1, we can see that the Cu(II)-coordinated quinone methide prefers to be protonated at the carboxylate but not at the 5/6-oxygen, in contrast to the case without Cu(II). These results clearly indicate that the Cu(II) coordination significantly inhibits O5/O6-protonation. This inhibition can be attributed to weakening the coordination between Cu(II) and the quinonoid oxygen by the protonation. As mentioned above, the unstable electronic structure formed by β-deprotonation would be stabilized by electrostatic attraction with negative charges of the quinonoid oxygens and positive charge of the Cu(II). This stabilization will be weakened by protonation to the quinonoid oxygen because protonation reduces the electron density localized around the oxygen nuclear by forming the O – H bond. Thus, we are able to see the clear difference between the two cases of with and without Cu(II) in dopachrome conversion. As the general implication for dopachrome conversion, it should be emphasized that the protection of quinonoid oxygens from protonations is important to form DHICA. Interestingly, this view is also applicable to the attempt to explain the preference of DHICA formation at strongly basic pH, which was experimentally confirmed [28]. Since basic pH conditions would contribute to inhibition of O6-protonation to the quinone methide intermediate as well as acceleration of α-deprotonation, we still can see the importance of the protection from quinonoid protonations in the discussion on the effect of pH.

3.4. Subsequent α-deprotonation to form DHICA

The carboxylate-protonated quinone methide, which is obtained by the inhibition of O5/O6-protonation by the Cu(II) coordination, must undergo α-deprotonation to form DHICA because decarboxylation is strongly blocked; the decarboxylation requires the dissociation of the carboxyl proton that would result in significant destabilization. This is our proposed mechanism of the selective formation of DHICA catalyzed by Cu(II). As shown in Fig. 7, we also confirm that the subsequent α-deprotonation from the carboxylate-protonated quinone methide

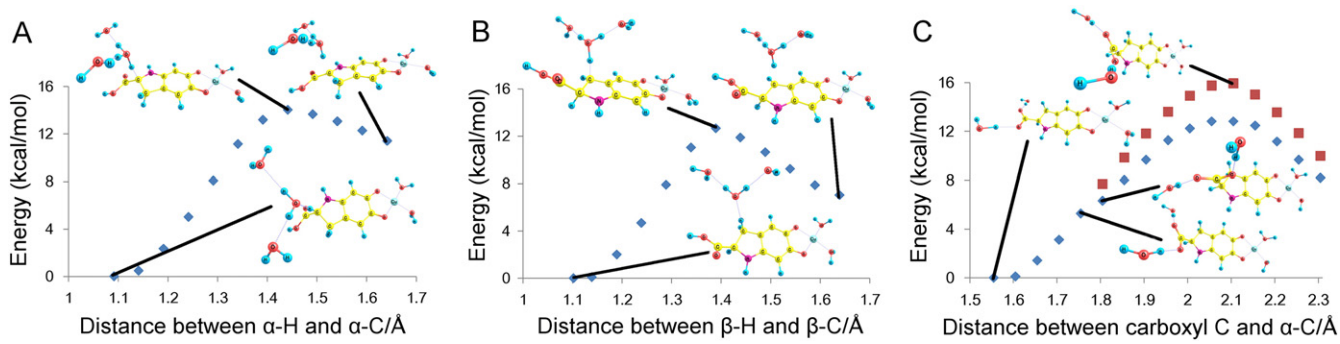

Fig. 5. Energy profiles for (A) α-deprotonation, (B) β-deprotonation, and (C) decarboxylation of dopachrome with Cu(II) coordination to quinonoid group. The diamonds in this figure C show the fully unrestricted relaxed potential energy curve for all degrees of freedom except for the distance of the cleaving C – C bond. The squares show the potential energy curve along the frozen dihedral angle around the cleaving C – C bond axis from before the non-smoothly changing point.

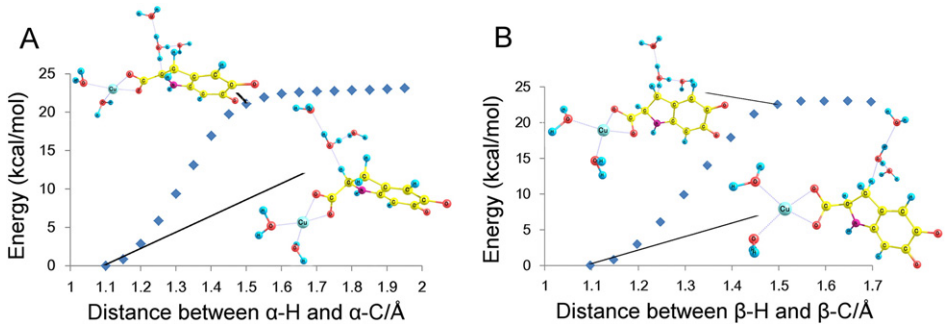

Fig. 6. Energy profiles for (A) α-deprotonation, (B) β-deprotonation of dopachrome with Cu(II) coordination to carboxylate group.

requires a comparatively low activation energy (9.832 kcal/mol) with respect to that of β-deprotonation. This low barrier indicates that β-deprotonation is the rate-limiting step in the dopachrome tautomerization to DHICA. As described in our previous work [43], β-deprotonation is rate-limiting also in the absence of Cu(II) coordination. Since deprotonations must be a base-catalyzed reaction, we can conclude that basic pH promotes dopachrome conversion both in the presence and in the absence of Cu(II). This conclusion is consistent with a recent experiment [35].

4. Conclusions

In this paper, we describe the mechanism of dopachrome tautomerization towards DHICA catalyzed by Cu(II) in aqueous solution. Despite the biological significance of this reaction and the existence of experimental data suggesting the strong catalytic behavior of Cu(II), the reaction mechanism of dopachrome tautomerization in the presence of Cu(II) has not been clarified. Our thoroughly examined model, in which Cu(II) is coordinated to quinonoid oxygens (5,6-oxygens) of dopachrome and two water molecules, enables us to give a simple but realistic view of the tautomerization at the atomic level. Based on numerical results from density functional theory-based calculation, we show that α-deprotonation, β-deprotonation, and decarboxylation, that are the important elementary steps to form DHICA, quinone methide intermediate, and DHI, respectively, are significantly activated by Cu(II) coordination to the quinonoid oxygens, corresponding to the catalytic behavior of Cu(II). In all three dissociations, the activation energy of β-deprotonation is evaluated to be the lowest value, indicating that the Cu(II)-catalyzed tautomerization of dopachrome also proceeds via the formation of quinone methide intermediate. Unlike the dopachrome conversion in the absence of Cu(II) which was investigated in our previous study [43], the quinone methide formed by β-deprotonation exhibits the preference of carboxylate protonation over quinonoid protonation, implying the inhibition of quinonoid protonation by the Cu(II) coordination. This inhibition can be attributed to weakening the coordination between Cu(II) and the quinonoid oxygen by the protonation. The subsequent α-deprotonation after proton rearrangement from β-carbon to carboxylate oxygen requires comparatively low activation energy with respect to that of β-deprotonation, indicating that β-deprotonation is the rate-limiting step in the dopachrome tautomerization to DHICA. We believe that these findings obtained here will be a guide for future studies towards unified understanding of dopachrome tautomerization to form DHICA which describes the details of the reaction catalyzed by not only Cu(II) but also other metal ions or DCT.

Supplementary data to this article can be found online at http://dx.doi.org/10.1016/j.bbagen.2014.10.024.

Table 1
Comparison of stability for each possible tautomer formed by a proton rearrangement from β-carbon of carboxyl-dissociated dopachrome in the presence/absence of Cu(II) coordination to quinonoid group.

Tautomer (Cu+/−)[a]	Reprotonated site[b]	Energy/ kcal·mol^{-1}[c]	Gibbs free energy/ kcal mol^{-1}[d]
Initial structure (Cu+)	β-Carbon	0.000	0.000
A (Cu+)	Carboxylate	−12.483	−12.451
B (Cu+)	O5	3.289	2.744
C (Cu+)	O6	8.302	7.088
Initial structure (Cu−)	β-Carbon	0.000	0.000
A (Cu−)	Carboxylate	11.282	11.384
B (Cu−)	O5	−5.695	−5.129
C (Cu−)	O6	1.822	1.929

[a] Symbols for tautomers formed by proton rearrangement from β-carbon of carboxyl-dissociated dopachrome. The presence and absence of Cu(II) coordination to quinonoid group are respectively denoted as (Cu+) and (Cu−).
[b] Numbers in this column correspond to the labels in Fig. 1 that follow usual chemical nomenclatures.
[c] Origins of energies evaluated with and without Cu(II) are respectively set to the values of carboxyl-dissociated dopachrome with and without Cu(II) before β-deprotonation.
[d] Origins of free energies evaluated with and without Cu(II) are respectively set to the values of carboxyl-dissociated dopachrome with and without Cu(II) before β-deprotonation. Temperature was set to 309.5 K as a condition of human body.

Acknowledgements

This work is supported in part by:
MEXT Grant-in-Aid for Scientific Research on Innovative Areas Program (2203–22104008) and Scientific Research (A) (26248006); JST ALCA Program "Development of Novel Metal-Air Secondary Battery Based on Fast Oxide Ion Conductor Nano Thickness Film"; JSPS Core-to-Core Program "A. Advanced Research Networks: Computational Materials Design on Green Energy"; and the Osaka University Joining and Welding Research Institute Cooperative Research Program.

Some of the numerical calculations presented here were done using the computer facilities at the following institutes: CMC (Osaka University), ISSP, KEK, NIFS, and YITP.

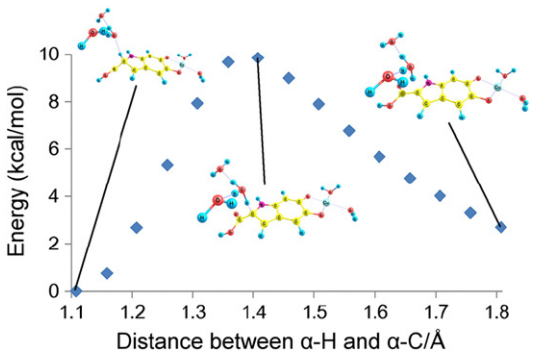

Fig. 7. Energy profile for α-deprotonation of carboxylate-protonated and β-deprotonated dopachrome with Cu(II) coordination to quinonoid group.

References

[1] M. Seiji, T.B. Fitzpatrick, R.T. Simpson, M.S.C. Birbeck, Chemical composition and terminology of specialized organelles (melanosomes and melanin granules) in mammalian melanocytes, Nature 197 (1963) 1082–1084.
[2] G. Raposo, M.S. Marks, Melanosomes — dark organelles enlighten endosomal membrane transport, Nat. Rev. Mol. Cell Biol. 8 (2007) 786–797.
[3] Y. Yamaguchi, M. Brenner, V.J. Hearing, The regulation of skin pigmentation, J. Biol. Chem. 282 (2007) 27557–27561.
[4] W.H. Tolleson, Human melanocyte biology, toxicology, and pathology, J. Environ. Sci. Health C Environ. Carcinog. Ecotoxicol. Rev. 23 (2005) 105–161.
[5] J.D. Simon, D.N. Peles, The red and the black, Acc. Chem. Res. 43 (2010) 1452–1460.
[6] J.D. Simon, D.N. Peles, K. Wakamatsu, S. Ito, Current challenges in understanding melanogenesis: bridging chemistry, biological control, morphology, and function, Pigment Cell Melanoma Res. 22 (2009) 563–579.
[7] S. Ito, K. Wakamatsu, Chemistry of mixed melanogenesis — pivotal roles of dopaquinone, Photochem. Photobiol. 84 (2008) 582–592.
[8] S. Ito, A chemist's view of melanogenesis, Pigment Cell Res. 16 (2003) 230–236.
[9] S. Ito, K. Wakamatsu, Human hair melanins: what we have learned and have not learned from mouse coat color pigmentation, Pigment Cell Melanoma Res. 24 (2010) 63–74.
[10] K. Wakamatsu, R. Kavanagh, A.L. Kadekaro, S. Terzieva, R.A. Sturm, S. Leachman, Z. Abdel-Malek, S. Ito, Diversity of pigmentation in cultured human melanocytes is due to differences in the type as well as quantity of melanin, Pigment Cell Res. 19 (2006) 154–162.
[11] T. Sarna, I.A. Menon, R.C. Sealy, Photosensitization of melanins: a comparative study, Photochem. Photobiol. 42 (1985) 529–532.
[12] L. Zecca, R. Pietra, C. Goj, C. Mecacci, D. Radice, E. Sabbioni, Iron and other metals in neuromelanins, substantia nigra, and putamen of human brain, J. Neurochem. 62 (1994) 1097–1101.
[13] R.J. D'Amato, Z.P. Lipman, S.H. Snyder, Selectivity of the Parkinsonian neurotoxin MPTP: toxic metabolite MPP^+ binds to neuromelanin, Science 231 (1986) 987–989.
[14] J.B. Nofsinger, Y. Liu, J.D. Simon, Aggregation of eumalanin mitigates photogeneration of reactive oxygen species, Free Radic. Biol. Med. 32 (2002) 720–730.
[15] J.M. Wood, K. Jimbow, R.E. Boissy, A. Slominski, P.M. Plonka, J. Slawinski, J. Wortsman, J. Tosk, What's the use of generating melanin? Exp. Dermatol. 8 (1999) 153–164.
[16] P. Meredith, J. Riesz, Radiative relaxation quantum yields for synthetic eumelanin, Photochem. Photobiol. 79 (2004) 211–216.
[17] J.B. Nofsinger, T. Ye, J.D. Simon, Ultrafast nonradiative relaxation dynamics of eumelanin, J. Phys. Chem. B 105 (2001) 2864–2866.
[18] J.B. Nofsinger, J.D. Simon, Radiative relaxation of *sepia* eumelanin is affected by aggregation, Photochem. Photobiol. 74 (2001) 31–37.
[19] J. Bustamante, L. Bredeston, G. Malanga, J. Mordoh, Role of melanin as a scavenger of active oxygen species, Pigment Cell Res. 6 (1993) 348–353.
[20] M. Tada, M. Kohno, Y. Niwano, Scavenging or quenching effect of melanin on superoxide anion and singlet oxygen, J. Clin. Biochem. Nutr. 46 (2010) 224–228.
[21] W. Korytowski, T. Sarna, Bleaching of melanin pigment: role of copper ions and hydrogen peroxide in autooxidation and photooxidation of synthetic dopa-melanin, J. Biol. Chem. 265 (1990) 12410–12416.
[22] P. Meredith, T. Sarna, The physical and chemical properties of eumelanin, Pigment Cell Res. 19 (2006) 572–594.
[23] M.L. Tran, B.J. Powell, P. Meredith, Chemical and structural disorder in eumelanins: a possible explanation for broadband absorbance, Biophys. J. 90 (2006) 743–752.
[24] P. Meredith, B.J. Powell, J. Riesz, S.P. Nighswander-Rempel, M.R. Pederson, E.G. Moore, Towards structure–property-function relationships for eumelanin, Soft Matter 2 (2006) 37–44.
[25] J.M. Pawelek, After dopachrome? Pigment Cell Res. 4 (1991) 53–62.
[26] M. Sugumaran, V. Semensi, Quinone methide as a new intermediate in eumelanin synthesis, J. Biol. Chem. 266 (1991) 6073–6078.
[27] H.S. Mason, The chemistry of melanin: III. Mechanism of the oxidation of dihydroxyphenylalanine by tyrosinase, J. Biol. Chem. 172 (1948) 83–99.
[28] K. Wakamatsu, S. Ito, Preparation of eumelanin-related metabolites 5,6-dihydroxyindole, 5,6-dihydroxyindole-2-carboxylic acid, and their *O*-methyl derivatives, Anal. Biochem. 170 (1988) 335–340.
[29] S. Ito, Reexamination of the structure of eumelanin, Biochim. Biophys. Acta 883 (1986) 155–161.
[30] S. Jiang, X. Liu, X. Dai, Q. Zhou, T. Lei, F. Beermann, K. Wakamatsu, S. Xu, Regulation of DHICA-mediated antioxidation by dopachrome tautomerase: implication for skin photoprotection against UVA radiation, Free Radic. Biol. Med. 48 (2010) 1144–1151.
[31] L. Panzella, A. Napolitano, M. d'Ischia, Is DHICA the key to dopachrome tautomerase and melanocyte functions? Pigment Cell Melanoma Res. 24 (2010) 248–249.
[32] D. Kovacs, E. Flori, V. Maresca, M. Ottaviani, N. Aspite, M.L. Dell'Anna, L. Panzella, A. Napolitano, M. Picardo, M. d'Ischia, The eumelanin intermediate 5,6-dihydroxyindole-2-carboxylic acid is a messenger in the cross-talk among epidermal cells, J. Invest. Dermatol. 132 (2012) 1196–1205.
[33] A. Palumbo, M. d'Ischia, G. Misuraca, G. Prota, Effect of metal ions on the rearrangement of dopachrome, Biochim. Biophys. Acta 925 (1987) 203–209.
[34] A. Palumbo, M. d'Ischia, G. Misuraca, G. Prota, T.M. Schultz, Structural modifications in biosynthetic melanins induced by metal ions, Biochim. Biophys. Acta 964 (1988) 193–199.
[35] S. Ito, N. Suzuki, S. Takebayashi, S. Commo, K. Wakamatsu, Neutral pH and copper ions promote eumelanogenesis after the dopachrome stage, Pigment Cell Melanoma Res. 26 (2013) 817–825.
[36] A.M. Körner, J. Pawelek, Dopachrome conversion: a possible control point in melanin biosynthesis, J. Invest. Dermatol. 75 (1980) 192–195.
[37] P. Aroca, J.C. García-Borrón, F. Solano, J.A. Lozano, Regulation of mammalian melanogenesis I: partial purification and characterization of a dopachrome converting factor: dopachrome tautomerase, Biochim. Biophys. Acta 1035 (1990) 266–275.
[38] F. Solano, C. Jiménez-Cervantes, J.H. Martínez-Liarte, J.C. García-Borrón, J.R. Jara, J.A. Lozano, Molecular mechanism for catalysis by a new zinc-enzyme, dopachrome tautomerase, Biochem. J. 313 (1996) 447–453.
[39] A. Palumbo, F. Solano, G. Misuraca, P. Aroca, J.C. García-Borrón, J.A. Lozano, G. Prota, Comparative action of dopachrome tautomerase and metal ions on the rearrangement of dopachrome, Biochim. Biophys. Acta 1115 (1991) 1–5.
[40] S. Commo, O. Gaillard, S. Thibaut, B.A. Bernard, Absence of TRP-2 in melanogenic melanocytes of human hair, Pigment Cell Res. 17 (2004) 488–497.
[41] S. Commo, K. Wakamatsu, I. Lozano, S. Panhard, G. Loussouarn, B.A. Bernard, S. Ito, Age-dependent changes in eumelanin composition in hairs of various ethnic origins, Int. J. Cosmet. Sci. 34 (2012) 102–107.
[42] S. Ito, Y. Nakanishi, R.K. Valenzuela, M.H. Brilliant, L. Kolbe, K. Wakamatsu, Usefulness of alkaline hydrogen peroxide oxidation to analyze eumelanin and pheomelanin in various tissue samples: application to chemical analysis of human hair melanins, Pigment Cell Melanoma Res. 24 (2011) 605–613.
[43] R. Kishida, Y. Ushijima, A.G. Saputro, H. Kasai, Effect of pH on elementary steps of dopachrome conversion from first-principles calculation, Pigment Cell Melanoma Res. 27 (2014) 734–743.
[44] P. Hohenberg, W. Kohn, Inhomogeneous electron gas, Phys. Rev. 136 (1964) B864–B871.
[45] W. Kohn, L.J. Sham, Self-consistent equations including exchange and correlation effects, Phys. Rev. 140 (1965) A1133–A1138.
[46] A.D. Becke, Density-functional thermochemistry. III. The role of exact exchange, J. Chem. Phys. 98 (1993) 5648–5652.
[47] C. Lee, W. Yang, R.G. Parr, Development of the Colle–Salvetti correlation-energy formula into a functional of the electron density, Phys. Rev. B 37 (1988) 785–789.
[48] M.J. Frisch, G.W. Trucks, H.B. Schlegel, G.E. Scuseria, M.A. Robb, J.R. Cheeseman, G. Scalmani, V. Barone, B. Mennucci, G.A. Petersson, H. Nakatsuji, M. Caricato, X. Li, H.P. Hratchian, A.F. Izmaylov, J. Bloino, G. Zheng, J.L. Sonnenberg, M. Hada, M. Ehara, K. Toyota, R. Fukuda, J. Hasegawa, M. Ishida, T. Nakajima, Y. Honda, O. Kitao, H. Nakai, T. Vreven, J.A. Montgomery Jr., J.E. Peralta, F. Ogliaro, M. Bearpark, J.J. Heyd, E. Brothers, K.N. Kudin, V.N. Staroverov, R. Kobayashi, J. Normand, K. Raghavachari, A. Rendell, J.C. Burant, S.S. Iyengar, J. Tomasi, M. Cossi, N. Rega, J.M. Millam, M. Klene, J.E. Knox, J.B. Cross, V. Bakken, C. Adamo, J. Jaramillo, R. Gomperts, R.E. Stratmann, O. Yazyev, A.J. Austin, R. Cammi, C. Pomelli, J.W. Ochterski, R.L. Martin, K. Morokuma, V.G. Zakrzewski, G.A. Voth, P. Salvador, J.J. Dannenberg, S. Dapprich, A.D. Daniels, Ö. Farkas, J.B. Foresman, J.V. Ortiz, J. Cioslowski, D.J. Fox, Gaussian 09, Revision C. 01, Gaussian, Inc., Wallingford CT, 2009.
[49] J. Tomasi, B. Mennucci, R. Cammi, Quantum mechanical continuum solvation models, Chem. Rev. 105 (2005) 2999–3093.
[50] J.L. Pascual-Ahuir, E. Silla, I. Tuñon, GEPOL: an improved description of molecular surfaces. III. A new algorithm for the computation of a solvent-excluding surface, J. Comput. Chem. 15 (1994) 1127–1138.
[51] A. Pasquarello, I. Petri, P.S. Salmon, O. Parisel, R. Car, É. Tóth, D.H. Powell, H.E. Fischer, L. Helm, A.E. Merbach, First solvation shell of the Cu(II) aqua ion: evidence for fivefold coordination, Science 291 (2001) 856–859.
[52] V.S. Bryantsev, M.S. Diallo, A.C.T. van Duin, W.A. Goddard III, Hydration of copper(II): new insights from density functional theory and the COSMO solvation model, J. Phys. Chem. A 112 (2008) 9104–9112.
[53] J.P. Foster, F. Weinhold, Natural hybrid orbitals, J. Am. Chem. Soc. 102 (1980) 7211–7218.